

Chronic mesothelial reaction and toxicity of potassium octatitanate fibers in the pleural cavity in mice and F344 rats

Masanao Yokohira, Yuko Nakano-Narusawa, Keiko Yamakawa, Nozomi Hashimoto, Shota Yoshida, Shohei Kanie and Katsumi Imaida

Onco-Pathology, Department of Pathology and Host-Defense, Faculty of Medicine, Kagawa University, Kita-gun, Kagawa, Japan

Key words

DHPN, mesothelioma, mouse, rat, TISMO

Correspondence

Katsumi Imaida, Onco-Pathology, Department of Pathology and Host-Defense, Faculty of Medicine, Kagawa University, 1750-1, Ikenobe, Miki-cho, Kita-gun, Kagawa 761-0793, Japan.

Tel: +81-87-891-2111; Fax: +81-87-891-2112;

E-mail: imaida@med.kagawa-u.ac.jp

Funding Information

No sources of funding were declared in this study.

Received December 20, 2015; Revised April 4, 2016;

Accepted April 9, 2016

Cancer Sci 107 (2016) 1047–1054

doi: 10.1111/cas.12944

Fiber-shaped particles of potassium octatitanate (tradename TISMO; chemical formula $K_2O \cdot 6TiO_2$), which are morphologically similar to asbestos particles, were shown to induce severe proliferative reactions in the pleural mesothelium in a previous experiment carried out over 21 weeks. The present study aims to determine whether these fibers induce malignant mesotheliomas in rodents, and to examine chronic toxicity induced. Additionally, we investigated the specific differences observable between the biological responses to the direct infusion of the fibers alone into the pleural cavity and those induced by the co-administration of the fibers with a known carcinogen. To detect the induction of malignant pleural mesotheliomas, two experiments were undertaken. In Experiment 1, four strains of mice, A/J, C3H, ICR, and C57BL, were examined for 52 weeks after experimental treatment with TISMO. In Experiment 2, the F344 rats were treated with TISMO alone, the lung carcinogen *N*-bis (2-hydroxypropyl) nitrosamine (DHPN) alone, both TISMO and DHPN, or left untreated and were then examined for 52 weeks. In this experiment, malignant lesion induction was expected in the co-administration group. TISMO fibers were observed in the alveoli, indicating penetration through the visceral pleura in mice and rats. The histopathological detection of TISMO fibers in the liver and kidneys of mice and rats indicated migration of the fibers out of the pleural cavity. Atypical mesothelial cells with severe pleural proliferation were observed, but malignant mesotheliomas were not detected. Among the rats, there were no observed malignant alterations in the mesothelium induced by DHPN–TISMO co-administration.

The incidence of pleural malignant mesotheliomas is increasing, particularly in less regulated countries^(1,2) and appropriate animal models for the same are necessary for the development of new therapeutic approaches. There have been reports of the induction of peritoneal mesotheliomas in rodents using chemicals or fibers,^(3–6) but pleural malignant mesotheliomas, more common than the peritoneal form in humans, are difficult to induce in rodents.⁽⁷⁾

In a previous study, we examined the effects of physical pulmonary collapse in mice by performing a thoracotomy followed by polymer gel infusion directly into the left cavity of the thorax.⁽⁸⁾ In this model, we observed pronounced mesothelial cell reactions on the left lung surfaces and parietal pleura. In an associated experiment,⁽⁹⁾ thoracotomy was followed by the separate infusion of three kinds of test particles directly into the pleural cavity of three groups of A/J mice (1.5 mg per 0.2 mL saline per mouse). These were fiber-shaped particles of potassium octatitanate (tradename TISMO, morphologically similar to asbestos), and granule-shaped micro-sized and nano-sized particles of titanium dioxide (TiO_2). After 21 weeks, only the TISMO fibers induced a severe reaction, with the

accumulation of iron derived from endogenous sources. The results indicated that the risk of adverse response in mesothelial cells depend not only on particle size but also on shape.

The objective of this study was to identify TISMO fiber-induced malignant mesotheliomas in rodents, if any, and to examine the pleural reaction to the fibers in a 1-year experimental period. In the present experiment, two studies, one to examine interstrain differences and the other to study interspecies differences, were used to confirm the presence or absence of induced malignant pleural mesotheliomas over a long observation period. In Experiment 1, interstrain effects of TISMO were studied over 52 weeks using A/J, C3H, ICR, and C57BL strains of mice. In Experiment 2, F344 rats treated with TISMO were examined for 52 weeks. Malignant mesothelioma induction by co-administration of TISMO with *N*-bis (2-hydroxypropyl) nitrosamine (DHPN), a lung carcinogen, was anticipated. We hypothesized that one of the mechanisms to induce malignant mesotheliomas might involve carcinogenic initiation by another agent in addition to direct stimulation by the fiber-shaped particles, especially in the case of epithelial-type malignant mesotheliomas.

Materials and Methods

Chemicals. Potassium octatitanate fibers (TISMO-D; chemical formula $K_2O \cdot 6TiO_2$) were supplied by Otsuka Chemical Co. Ltd. (Osaka, Japan) as fibers with length (mean dimension) $<50 \mu\text{m}$ and width $<2 \mu\text{m}$. We had confirmed these dimensions in previous work using scanning electron microscope imaging of the TISMO fibers.⁽⁹⁾ The mean length and width of the 21 counted TISMO fibers on the previously obtained scanning electron microscope image were $16.6 \pm 10.5 \mu\text{m}$ (average \pm SD) and $0.7 \pm 0.9 \mu\text{m}$, respectively. For administration, the fibers were suspended in saline (isotonic sodium chloride solution; Otsuka Pharmaceutical Factory, Inc., Tokushima, Japan). Three milligrams of TISMO particles suspended in 0.2 mL saline showed both aggregated TISMO fibers as well as separated single fibers.⁽¹⁰⁾ *N*-bis (2-hydroxypropyl) nitrosamine (Nacalai Tesque Inc., Kyoto, Japan) was used to induce lung tumorigenesis in Experiment 2.

Animals. A/J (A/JJmsSlc) and C3H (C3H/HeNSlc) mice were purchased from Japan SLC, Inc. (Shizuoka, Japan). ICR (CrI:CD1) and C57BL (C57BL/6J) mice and F344 (F344/DuCrIcrj) rats were from Japan Charles River (Shiga, Japan). The mice were female and 5 weeks of age at arrival; the rats were male and 4 weeks of age. The animals were maintained in the Division of Animal Experiments, Life Science Research Center, Kagawa University (Kagawa, Japan), according to the Institutional Regulations for Animal Experiments. The regulations included the best considerations on animal welfare and good practices in animal handling including the replacement, refinement, and reduction of animal testing. The protocols used for these experiments were approved by the Animal Care and Use Committee of Kagawa University. The animals were housed in polycarbonate cages on bedding consisting of recycled paper chips (EchoChip, CL-4163; CLEA Japan, Inc., Tokyo, Japan) and maintained under controlled conditions of humidity ($60 \pm 10\%$), lighting (12:12 h light:dark cycle), and temperature ($24 \pm 2^\circ\text{C}$). The animals were given free access to drinking tap water and a basal diet of Oriental MF (Oriental Yeast Co., Ltd., Tokyo, Japan) for mice and CE-2 (CLEA Japan Inc., Tokyo, Japan) for rats. The animals were acclimated for 2 weeks prior to the start of the experiments described below.

Experimental design. *Experiment 1.* Groups were formed from 144 seven-week-old mice. The eight groups consisted of four groups of 30 mice each and another four groups of six mice each (groups 1–8). Groups 1 and 5 consist of A/J mice, groups 2 and 6 comprise ICR mice, groups 3 and 7 include C3H mice, and groups 4 and 8 have C57BL mice. Groups 1–4 were TISMO-treated groups and groups 5–8 were sham-operated groups. At the beginning of the experiment, all mice from groups 1–8 underwent a left thoracotomy, with those of groups 1–4 treated with 3 mg TISMO suspended in 0.2 mL saline per mouse directly into the left pleural cavity. Under deep anesthesia, a skin incision (approximately 7 mm long) was made on the left axilla. After confirmation of the location of the thoracic wall, thoracotomy was completed with an incision (approximately 5 mm long) between ribs. The left lung was observed directly through the opened hole and atelectasis was confirmed. After infusion of the test solutions into the left pleural cavity for groups 1–4 (no infusion for groups 5–8), the skin was clipped together to close the thorax. Of the TISMO-treated mice, 28 (nine of group 1; two of group 2; four of group 3; and 13 of group 4) died just after treatment; these mortalities were presumed to be the result of surgery and/or

anesthesia. The experiment was terminated at 415 days after surgery for the decrease in effective number, when all surviving animals were killed under deep anesthesia.⁽⁹⁾

Experiment 2. Groups were formed from 46 six-week-old rats. The four groups consisted of 15, 15, 11, and 5 rats each (groups 1–4, respectively). At the beginning of the experiment, rats from groups 1 and 2 were given 0.1% DHPN in drinking water for 2 weeks. Rats from groups 1 and 3 were given 30 mg TISMO suspended in 2 mL saline per rat in the fourth week. The operation for TISMO treatment to rats followed the same procedure adopted in mice. Group 2 was a DHPN control group and group 4 an untreated control group. No rat died during TISMO treatment. All rats were killed at 52 weeks after surgery.

Tissue preparation. At necropsy, the lungs with visceral pleura, the liver, and the kidneys were removed and, if some other pathology was grossly observed, the relevant organ was also removed. If thickening of the parietal pleura was observed, the lesion was excised along with the chest wall, including the ribs and intercostal muscle. The removed organs were weighed, but the lungs in Experiment 1 could not be weighed successfully due to severe adhesions. Other organs were fixed and processed for histopathological evaluation of HE stained sections. Specifically, organs were immersed in 10% neutral buffered formalin for 3 days, following which two longitudinal slices from the left lobe of the lung and one orthogonally oriented hilum slice from each of the right lobes of the lung were processed for embedding in paraffin. When lung nodules were observed by gross inspection, additional slices were processed to allow histopathological assessment. Lung lesions were categorized as bronchioloalveolar adenomas and bronchioloalveolar adenocarcinomas in accordance with the established criteria provided in the International Harmonization of Nomenclature and Diagnostic Criteria.⁽¹¹⁾ The diagnosis of mesothelial lesions was also carried out according to this criteria. Pleural findings were examined and the parameters of maximum pleural thickness, number of mitoses, pleural cell atypia, and inflammatory cell infiltration were assessed. Maximum pleural thickness was measured and its relative value was calculated using body weight. The number of mitoses in each HE section was counted in the pleura in a whole slide. Atypia and inflammatory cells were scored as follows: 0, none; 1, mild; 2, moderate; and 3, severe.

In addition, immunostaining of calretinin and napsin A was carried out to identify mesothelial cells and lung epithelial tumors in the lung.^(12,13) Lungs were immunostained by the avidin–biotin complex method. All staining processes from deparaffinization to counterstaining with hematoxylin were undertaken automatically using the Leica BOND-III staining system (Leica Biosystems, Nussloch, Germany). Antigen retrieval was not undertaken for calretinin or napsin A. The anti-mouse calretinin mAb (clone 5A5), purchased from Novocastra Laboratories (Newcastle Upon Tyne, UK), was used at 1:100 dilution. The anti-mouse napsin A mAb (NCL-L-Napsin A) was purchased from Leica Microsystems Newcastle Ltd. (Newcastle Upon Tyne, UK) was used at 1:100 dilution. The reaction time for each primary antibody was 15 min.

To detect the fibers, polarized light microscopy was used for screening purposes. A BX51 microscope equipped with the Olympus Polarizer for Transmitted Light (U-P110; Olympus, Tokyo, Japan) was used.

Statistical analysis. Data for body and organ weights were analyzed using the Tukey–Kramer test (multiple comparison test). Fisher's exact probability test was used to analyze

increases in incidence in macroscopic and histopathological data.

Results

Experiment 1. Some mice were found dead before the end of the experimental period, although the general condition of rodents in all the groups showed no remarkable change. Immediately after the operation, 28 mice died. The final numbers of mice under observation were 13 in group 1, 23 in group 2, 13 in group 3, 10 in group 4, six in group 5, five in group 6, six in group 7, and six in group 8. Due to increasing mortality in group 4, the remaining mice were killed on day 415. Final body and organ weights are shown in Table 1. There was no significant difference in body weights and absolute (data is not shown) and relative weights (body weight-normalized) of the liver and kidneys between the TISMO-treated and control groups belonging to the same strain. Due to exfoliation and severe adhesion to the thorax, lung weights were too low for reliable use as relative values.

At autopsy, some of the mice in groups 2 and 4 showed gross hypertrophy of the liver and the occurrence of ascites (Table 2). In all the mice of TISMO-treated groups 1–4, the infused fibers formed discrete masses in the thoracic cavity, with severe adhesions attaching the left lung (especially the left lobe) to the thorax. The right lung showed slight or no adhesion to the surrounding tissue and adequate expandability. In Groups 2 and 4, nodules were observed in other organs, diagnosed histopathologically as serous adenoma of the ovary, sarcoma of the uterus, and calcifying epithelioma of the skin.

Table 1. Body weights and relative weights of liver and kidneys in four strains of mice treated with potassium octatitanate fibers (TISMO) (Experiment 1)

Group	Strain	TISMO	No.†	Body weight, g	Liver, %	Kidneys, %
1	A/J	+	12	28.6 ± 5.5	4.0 ± 0.3	1.1 ± 0.1
2	ICR	+	22	50.2 ± 10.5	3.7 ± 0.9	0.9 ± 0.3
3	C3H	+	7	24.6 ± 3.1	3.9 ± 0.5	1.1 ± 0.1
4	C57BL	+	9	31.0 ± 7.2	3.8 ± 0.7	0.9 ± 0.2
5	A/J	–	5	32.7 ± 3.8	3.5 ± 0.1	1.0 ± 0.1
6	ICR	–	5	53.8 ± 15.5	3.7 ± 0.6	0.8 ± 0.1
7	C3H	–	6	25.2 ± 2.5	4.4 ± 0.7	1.1 ± 0.1
8	C57BL	–	6	36.6 ± 5.8	3.7 ± 0.8	0.7 ± 0.2

There are no significant differences between groups treated with TISMO (+) or not (–) in the same strain. †Effective number of mice.

Table 2. Macroscopic findings in four strains of mice treated with potassium octatitanate fibers (TISMO) (Experiment 1)

Group	Strain	TISMO	No.†	Ascites	Liver hypertrophy	Ovary nodule	Uterus nodule	Skin nodule
1	A/J	+	11	0	0	0	0	0
2	ICR	+	22	4	4	2‡	0	1§
3	C3H	+	7	0	0	0	0	0
4	C57BL	+	9	1	1	0	1¶	1
5	A/J	–	5	0	0	0	0	0
6	ICR	–	5	0	0	0	0	0
7	C3H	–	6	0	0	0	0	0
8	C57BL	–	6	0	0	0	0	0

†Effective number of mice. ‡Serous adenoma. §Calcifying epithelioma. ¶Sarcoma. +, Treated with TISMO; –, untreated.

There were no intergroup differences in the incidence of the lesions. The histopathological findings are summarized in Table 3. Bronchioloalveolar adenomas and adenocarcinomas were observed, but no significant intergroup differences in incidence or multiplicity of these nodules was seen. Pleural thickening, characterized by chronic inflammation, prominent fibrosis of the lungs, and infolding of the pleura into the lungs (Fig. 1b), were observed in all TISMO treated mice (groups 1–4, Table 2 and Fig. 1a–d). Several TISMO fibers, in aggregated or isolated forms, were observed in the alveoli, indicating an ability of the fibers to penetrate the pleura.

Detailed findings regarding the pleura are summarized in Table 4. ICR mice treated with TISMO (group 2) showed significantly weaker thickening in the pleura than all the other TISMO-treated groups. C57BL mice showed an increase in occurrence of mitoses, and A/J mice displayed severe atypia of pleural cells. Inflammation accompanied by prominent fibrosis was limited to the pleura, but this finding could not be considered a diagnosis for malignant mesothelioma. Inflammatory cell foci, characterized by macrophages, plasma cells, lymphocytes, and a small number of leukocytes, were observed in the lungs and pleura of 19 mice of group 2, three of group 4, and two of group 8. Several macrophages were observed in the thickening pleura, some of which ingested the fibers completely, while others could not ingest the entire length.

The fibers were also detected histopathologically in the liver and kidneys. In the liver, inflammatory cell infiltration was observed around the fibers crossing into the portal area (Fig. 1e,f) and TISMO fibers on the surface caused fibrosis (Fig. 1g). In the kidney, TISMO fibers were detected mainly in the glomeruli under polarized light microscopy but the renal tissues did not show inflammation (Fig. 1h).

Experiment 2. No rat was killed during TISMO treatment. The animals in all groups showed no remarkable change in their general condition during the experimental period. From day 262 onwards, increasing mortality was observed in groups 1 and 2 (DHPN treated). All the rats were killed 52 weeks following treatment and the final numbers of the rats were 10 in group 1, 11 in group 2, 11 in group 3, and five in group 4. Final body and organ weights are shown in Table 5. The average body weights of the DHPN-treated groups (groups 1 and 2) were significantly decreased compared with those of the untreated group (group 4). The relative weights of the lungs in groups 1 and 2 were significantly increased compared with those in groups 3 and 4.

At necropsy, whitish nodules were grossly observed in the lungs of rats of groups 1 and 2. The infused TISMO fibers were associated with discrete masses and severe adhesions around the

Table 3. Histopathological findings in four strains of mice treated with potassium octatitanate fibers (TISMO) (Experiment 1)

Group	Strain	TISMO	No.†	Ascites	Lung		Liver		Kidney
					Bronchioloalveolar adenocarcinoma	Bronchioloalveolar adenoma	TISMO on surface	Inflammatory cell foci	Inflammatory cell foci
1	A/J	+	11	0	0	0	0	0	0
2	ICR	+	22	4	2	0	6	1	0
3	C3H	+	7	0	0	0	0	0	0
4	C57BL	+	9	1	0	0	2	4	0
5	A/J	-	5	0	0	3	0	0	1
6	ICR	-	5	0	0	0	0	0	0
7	C3H	-	6	0	0	0	0	0	0
8	C57BL	-	6	0	0	0	0	6	0

†Effective number of mice. +, Treated with TISMO; -, untreated.

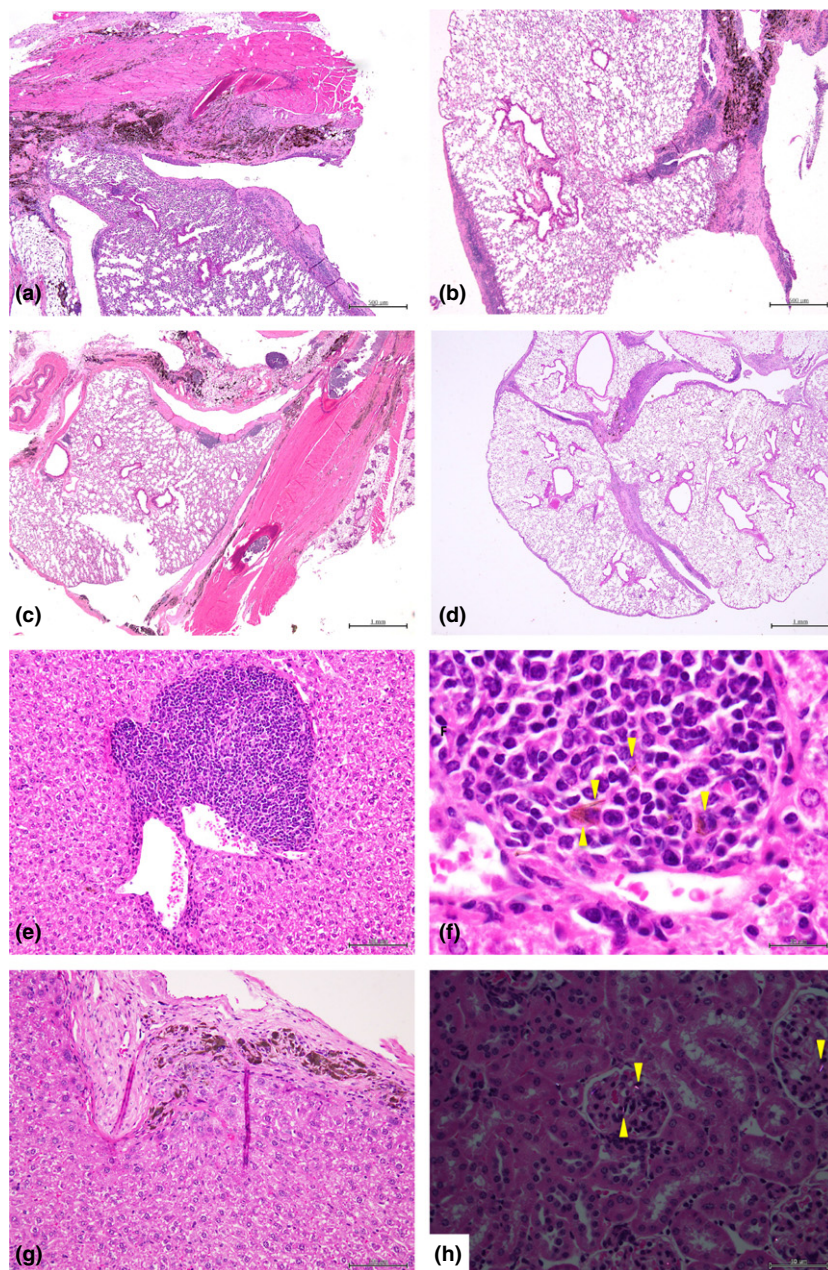


Fig. 1. Histopathological findings on day 415 for mice treated with potassium octatitanate fibers (TISMO) (groups 1–4; Experiment 1). Lungs from A/J mice (group 1) (a), ICR mice (group 2) (b), C3H mice (group 3) (c), and C57BL mice (group 4) (d) with HE staining. Livers from C57BL mice (group 4) (e, f) and ICR mice (group 2) (g). (h) Kidneys from C57BL mice (group 4). Pleural thickening of the lungs and infolding of the pleura into the lungs (b) were observed in all mice of the TISMO-treated groups (a–d). Fibers were detected in the liver and kidneys, despite TISMO infusion only into the pleural cavity (e, f, yellow arrows). In the liver, inflammatory cell infiltration was observed around the fibers in the portal area (e, f) and TISMO fibers on the surface caused fibrosis (g). TISMO fibers were detected mainly in the glomeruli under polarized light microscopy but the renal tissues did not show inflammation (h).

Table 4. Pleural findings in four strains of mice treated with potassium octatitanate fibers (TISMO) (Experiment 1)

Group	Strain	TISMO	No.†	Pleural thickening			Pleural findings		
				Incidence	Absolute, mm	Relative, mm/kg B.W.	Number of mitosis‡	Atypia§	Inflammatory cells§
1	A/J	+	11	100 (11/11)	0.6 ± 0.2	22.4 ± 8.0	0.2 ± 0.4	2.7 ± 0.5*	0.6 ± 0.7
2	ICR	+	22	100 (22/22)	0.4 ± 0.3	8.5 ± 5.8**	0.1 ± 0.3	2.3 ± 0.8	1.1 ± 0.8
3	C3H	+	7	100 (7/7)	0.7 ± 0.2	27.6 ± 7.6	0.3 ± 0.5	2.1 ± 0.4	0.9 ± 0.7
4	C57BL	+	9	100 (9/9)	0.6 ± 0.3	20.7 ± 11.6	0.4 ± 0.7	1.9 ± 0.3	2.0 ± 0.7***
5	A/J	–	5	0 (0/0)	0.0 ± 0.0	0.0 ± 0.0	0.0 ± 0.0	0.0 ± 0.0	0.6 ± 0.5
6	ICR	–	5	0 (0/0)	0.0 ± 0.0	0.0 ± 0.0	0.0 ± 0.0	0.0 ± 0.0	0.2 ± 0.4
7	C3H	–	6	0 (0/0)	0.0 ± 0.0	0.0 ± 0.0	0.0 ± 0.0	0.0 ± 0.0	0.0 ± 0.0
8	C57BL	–	6	0 (0/0)	0.0 ± 0.0	0.0 ± 0.0	0.0 ± 0.0	0.0 ± 0.0	0.2 ± 0.4

* $P < 0.05$ vs group 4. ** $P < 0.05$ vs groups 1, 2, and 4. *** $P < 0.05$ vs groups 1, 2, and 3. †Effective number of mice. ‡Counted in pleura of left lobe of specimen. §Scored as: 0, none; 1, mild; 2, moderate; 3, severe. +, Treated; –, untreated. B.W., body weight.

Table 5. Body weights and relative weights of lung, liver, and kidneys in rats treated with potassium octatitanate fibers (TISMO) and/or *N*-bis (2-hydroxypropyl) nitrosamine (DHPN) (Experiment 2)

Group	DHPN	TISMO	No.†	Body weight, g	Lung, %	Liver, %	Kidneys, %	
							Right	Left
1	+	+	10	347.8 ± 39.1***	0.9 ± 0.2***	2.5 ± 0.1	0.3 ± 0.0	2.3 ± 5.2
2	+	–	11	351.7 ± 48.2**	0.7 ± 0.3***	2.5 ± 0.1	1.4 ± 3.7	0.3 ± 0.0
3	–	+	11	392.7 ± 21.1	0.4 ± 0.1	2.6 ± 0.2	0.3 ± 0.0	0.3 ± 0.0
4	–	–	5	404.2 ± 18.8	0.4 ± 0.1	2.6 ± 0.1	0.3 ± 0.0	0.3 ± 0.0

* $P < 0.05$ vs group 3. ** $P < 0.05$ vs group 4. †Effective number of rats. +, Treated; –, untreated.

Table 6. Histopathological findings in rats treated with potassium octatitanate fibers (TISMO) and/or *N*-bis (2-hydroxypropyl) nitrosamine (DHPN) (Experiment 2)

Group	DHPN	TISMO	No.†	Lung proliferative lesions			
				Incidence, %		Multiplicity	
				Tumor‡	Bronchioloalveolar adenocarcinoma	Tumor	Bronchioloalveolar adenocarcinoma
1	+	+	10	100 (10/10)	80 (8/10)	9.7 ± 4.5	2.5 ± 2.1
2	+	–	11	100 (11/11)	90.9 (10/11)	9.5 ± 2.8	2.5 ± 1.4
3	–	+	11	0 (0/11)	0 (0/11)	–	–
4	–	–	5	0 (0/5)	0 (0/5)	–	–

There are no intergroup significant differences in tumor or carcinoma incidence between groups 1 and 2 by Tukey–Kramer test. †Effective number of rats. ‡Bronchioloalveolar adenoma + bronchioloalveolar adenocarcinoma. +, Treated; –, untreated.

left lobes of the lungs in all the TISMO-treated rats (groups 1 and 3). Some rats with swellings or nodules in the kidney were observed in DHPN-treated groups (groups 1 and 2).

The incidences and multiplicities of the histopathological findings in the lungs are summarized in Table 6. The macroscopic lung nodules were confirmed to be bronchioloalveolar adenomas or adenocarcinomas, but significant differences in incidence of proliferative lesions were not observed between groups 1 and 2. In rats from TISMO-treated groups 1 and 3, pleural thickening and atypical cells were observed in the lung (Fig. 2). Lesions invading the lung in rats from group 1 were observed but could not be used as diagnoses for mesothelioma or bronchioloalveolar adenocarcinoma (Fig. 2a,b). Therefore, immunohistochemical analyses for calretinin and napsin A were undertaken. The atypical cells in the lesion were positive

for napsin A (Fig. 2c) and negative for calretinin (Fig. 2d). From these results, the rats could be diagnosed with bronchioloalveolar adenocarcinoma.

Pleural thickening results are summarized in Table 7. There were no significant intergroup differences between groups 1 and 3, and no influence of DHPN on the pleural thickening can be inferred. The TISMO fibers were administered directly into the thoracic cavities, but fibers were also detected in the kidneys and livers of all the rats of the TISMO-treated groups (groups 1 and 3). Reactions such as inflammatory cell infiltration in response to TISMO fibers were not observed in the liver and kidneys.

In the kidneys of DHPN-treated groups (groups 1 and 2), nephroblastoma, renal cell carcinoma, and urothelial carcinoma (renal pelvic carcinoma) were observed but there was no

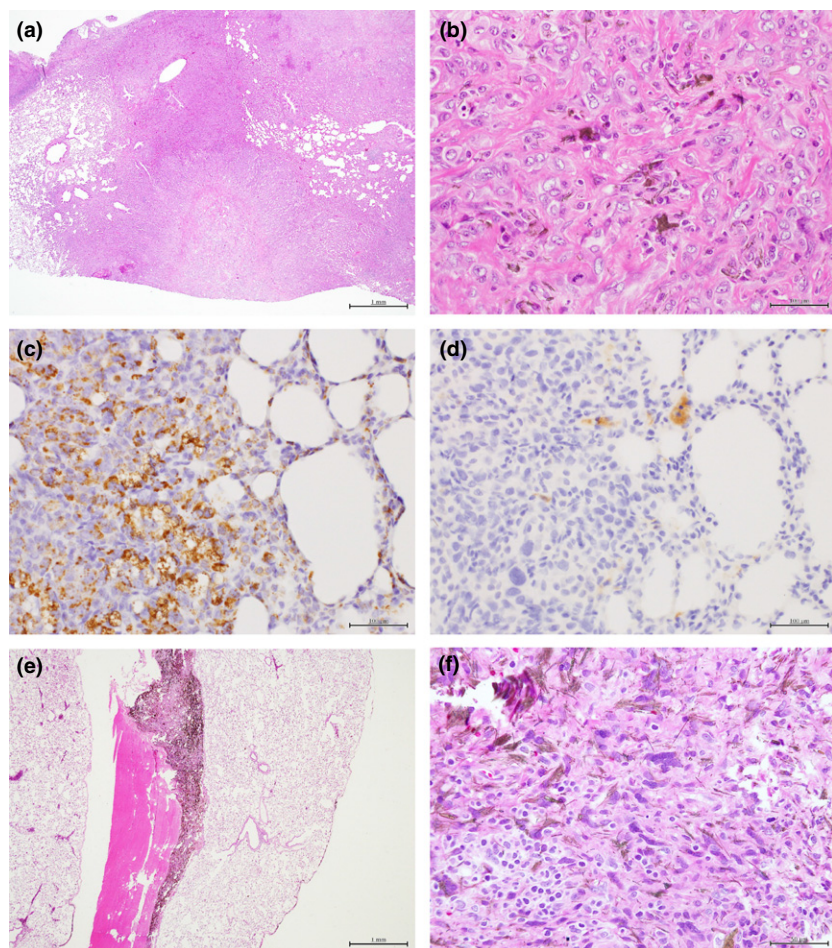


Fig. 2. Histopathological findings at week 52 for rats treated with potassium octatitanate fibers (TISMO) (Experiment 2). (a, b) Lungs from Group 1 rats (treated with TISMO and N-bis (2-hydroxypropyl) nitrosamine (DHPN)) with HE staining. (b) Lungs from group 2 rats (DHPN only). (c) Lungs from group 1 rats (DHPN and TISMO) with immunohistochemical staining for napsin A. (d) Lungs from group 1 rats (DHPN and TISMO) with immunohistochemical staining for calretinin. (e, f) Lungs from group 3 rats (TISMO only). In TISMO-treated groups 1 and 3, pleural thickening and atypical cells were observed in the lung (a, b, e, f). The invasive lesions in the lung of group 1 were observed but could not be distinguished as either mesotheliomas or bronchioloalveolar adenocarcinomas (a, b). The atypical cells in the lesions stained positive for napsin A (c) and negative for calretinin (d).

Table 7. Pleural findings in rats treated with potassium octatitanate fibers (TISMO) and/or N-bis (2-hydroxypropyl) nitrosamine (DHPN) (Experiment 2)

Group	DHPN	TISMO	No.†	Pleural thickening		
				Incidence, %	Absolute, mm	Relative, mm/kg B.W.
1	+	+	10	100 (10/10)	0.47 ± 0.16	1.40 ± 0.61
2	+	–	11	0 (0/11)	0.04 ± 0.05	0.13 ± 0.17
3	–	+	11	100 (11/11)	0.55 ± 0.23	1.42 ± 0.57
4	–	–	5	0 (0/5)	0.02 ± 0.04	0.05 ± 0.11

There are no intergroup significant differences between groups 1 and 3 by Tukey–Kramer test. †Effective number of rats. +, Treated; –, untreated. B.W., body weight.

significant difference in incidence between groups 1 and 2 (data is not shown).

Discussion

The present study shows that long-term exposure to TISMO fibers, morphologically similar to asbestos particles, when infused into the pleural cavity, results in pleural thickening, characterized by chronic inflammation and prominent fibrosis of the lungs, in all strains of mice and rats. Respiratory exposure to asbestos is associated with mesotheliomas in humans

and electron spin resonance analyses have shown that crocidolite and amosite contain high amounts of iron.⁽¹⁴⁾ Although the chemical formula of TISMO used in the present experiments is $K_2O \cdot 6TiO_2$, indicating that it does not contain a ferrous component, intraperitoneal or intrascrotal application of multiwall carbon nanotube, also without any ferrous component, has been reported to induce mesotheliomas.^(15,16)

In Experiment 1, some mice were found dead before the end of the experimental period, although the general condition of animals in all groups showed no remarkable change. In order to induce malignant lesions, a longer experimental period was desirable. However, due to increasing mortality of C57BL mice in group 4, all mice were killed on day 415. A previous experiment using A/J mice with potential for a long experimental period was terminated on day 457, also due to increasing mortality.⁽¹⁰⁾ The shorter period of the present experiment, 415 days, appears to be due to the strain difference.

Histopathological examination revealed pleural thickening, characterized by chronic inflammation and prominent fibrosis of the lungs, and infolding of the pleura into the lungs were observed in all mice of the TISMO-treated groups (groups 1–4). However, inflammatory responses accompanied by prominent fibrosis were limited to the pleura, so this finding could not be used as a diagnosis for malignant mesothelioma. Our previous 21-week experiment to examine the differences in effects among various strains of mice showed that inflammatory cell infiltration into thickened pleura induced by TISMO was significant in the lungs of ICR mice.⁽¹⁷⁾ The present

experiment, carried out over a longer period, was to examine the potential pleural tumorigenesis, but no induced malignant mesothelioma was observed. However, TISMO-treated mice responded differently based on strain, with mild thickening and increased inflammatory cell infiltration observed in ICR mice, and severe atypia of cells in A/J mice. The findings are complex and it is difficult to explain the mechanism of action of the TISMO fibers. However, ICR mice seemed to show milder responses, hinting at a species with potential for resistance to proliferative effects of fiber-shaped particles. Moreover, inflammatory cell infiltration in the pleura could contribute to the inhibition of fiber-induced pleural thickening.

The fibers were also detected histopathologically in the liver and kidneys of all strains of mice in Experiment 1. In our previous 457-day experiment using A/J mice, we reported histopathological detection of fibers in several organs, including the liver, kidneys, spleen, heart, ovaries, bone marrow, and brain.⁽¹⁰⁾ The route to these other organs from the pleural cavity is suspected to be through blood vessels because the fibers were detected in the glomeruli of the kidney, in and around the vessels in the liver and brain, and in the bone marrow and spleen. However, it remains unclear whether these vessels provide the only route to remote organs. Generally, a proportion of all particles that are deposited in the peripheral lung are reported to travel through to the pleura and exit through the stomata in the parietal pleura to the underlying lymphatic system and subsequently to the mediastinal lymph nodes.^(18,19) TISMO on the surface of the liver in the presently discussed Experiment 1 is considered to have arrived directly from the pleural cavity through the diaphragm.

The rats in Experiment 2 were expected to develop malignant lesions due to co-treatment with TISMO and DHPN. A lung carcinogen⁽²⁰⁾ used for tumor initiation, DHPN is reported to be associated with activating mutations of the *Kras* gene at codon 12 in 47% of rat lung neoplastic lesions.⁽²¹⁾ It is also known to be a carcinogen targeting the thyroid gland, urinary bladder, and kidneys.^(22–24) The kidneys of DHPN-treated groups in Experiment 2 showed nephroblastoma, renal cell carcinoma, and urothelial carcinoma (renal pelvic carcinoma), which were suspected to have been initiated and induced by DHPN.

Histopathologically speaking, the lesions invading the lungs of group 1 rats (TISMO + DHPN) were observed, but could not be distinguished as either mesotheliomas or bronchioloalveolar adenocarcinomas. To address this, immunohistochemical analysis for calretinin and napsin A was carried out. Napsin A is an aspartic proteinase involved in the maturation of surfactant protein-B (SP-B),⁽²⁵⁾ expressed in the cytoplasm

of type II pneumocytes and Clara cells in the lung.^(26–28) As used in human clinical studies, napsin A is a highly specific marker for bronchioloalveolar adenocarcinomas in the lung.^(29,30) Calretinin is reported to be a useful marker for the positive identification of malignant mesotheliomas.⁽³¹⁾ In the present experiment, the atypical cells in the lesion were positive for napsin A and negative for calretinin, meaning that the lesions originated not from a mesothelioma, but from a bronchioloalveolar adenocarcinoma. Experiment 2 was undertaken to examine the interaction between DHPN and the mesothelial reaction to TISMO treatment, as well as to examine rats for TISMO-induced toxicity. However, neither was there any observed malignant alteration to the TISMO-induced mesothelial reaction caused by DHPN treatment, nor did TISMO promote DHPN-induced lung tumor. This result suggests that lung tumor induced by DHPN and mesothelial reaction to TISMO fibers possess independent actions.

In the two experiments, malignant mesothelioma was not observed, even though the experiments were designed in anticipation of its development. One of the possible reasons could involve the aggregation of TISMO fibers in the pleural cavity. While separated single fibers in HE-stained lung specimens were observed, single fibers were less abundant than aggregated fibers. Fibrous nanomaterial such as multiwall carbon nanotube is reported to be a mixture of dispersed single fibers of various lengths and widths, as well as their agglomerates and aggregates.⁽³²⁾ When given as a mixture, the lung lesions were mainly seen as inflammatory and/or granulomatous lesions accompanying the aggregates and were considered as blocking and/or masking the changes induced by the single fibers that should have reached the alveolar ducts and alveoli.⁽³²⁾ Preparing a dispersed single fiber TISMO solution without aggregates or agglomerates may be expected to induce malignant mesothelioma.

In conclusion, this study showed that the intrathoracic infusion of TISMO fiber did not cause malignant mesothelioma in multiple strains of mice and rats, but severe chronic inflammation and proliferation of pleural mesothelial cells were observed. Asbestos-like fibers may, however, spread from the pleural cavity to other sites of the liver and kidneys regardless of strain or species. These results may serve as important information when considering future hazard risks in the use of this type of particle.

Disclosure Statement

Katsumi Imaida receives research funding from Taiho Pharmaceutical Co., Ltd.

References

- Metintas S, Metintas M, Ucgun I, Oner U. Malignant mesothelioma due to environmental exposure to asbestos: follow-up of a Turkish cohort living in a rural area. *Chest* 2002; **122**: 2224–9.
- Robinson BW, Musk AW, Lake RA. Malignant mesothelioma. *Lancet* 2005; **366**: 397–408.
- Kim Y, Ton TV, DeAngelo AB et al. Major carcinogenic pathways identified by gene expression analysis of peritoneal mesotheliomas following chemical treatment in F344 rats. *Toxicol Appl Pharmacol* 2006; **214**: 144–51.
- Kamstrup O, Ellehauge A, Collier CG, Davis JM. Carcinogenicity studies after intraperitoneal injection of two types of stone wool fibres in rats. *Ann Occup Hyg* 2002; **46**: 135–42.
- Krajnow A, Lao I. Assessment of carcinogenic effect of aluminosilicate ceramic fibers produced in Poland. Animal experiments. *Med Pr* 2000; **51**(1): 19–27.
- Crosby LM, Morgan KT, Gaskill B, Wolf DC, DeAngelo AB. Origin and distribution of potassium bromate-induced testicular and peritoneal mesotheliomas in rats. *Toxicol Pathol* 2000; **28**: 253–66.
- Moore AJ, Parker RJ, Wiggins J. Malignant mesothelioma. *Orphanet J Rare Dis* 2008; **3**: 34.
- Yokohira M, Hashimoto N, Yamakawa K, Saoo K, Kuno T, Imaida K. Lack of promoting effects from physical pulmonary collapse in a female A/J mouse lung tumor initiated with 4-(methylnitrosamino)-1-(3-pyridyl)-1-butanone (NNK) with remarkable mesothelial cell reactions in the thoracic cavity by the polymer. *Exp Toxicol Pathol* 2011; **63**: 181–5.
- Yokohira M, Hashimoto N, Yamakawa K et al. Potassium octatitanate fibers (TISMO) induce pleural mesothelial cell reactions with iron accumulation in female A/J mice. *Oncol Lett* 2010; **1**: 589–94.
- Yokohira M, Hashimoto N, Nakagawa T et al. Long-term chronic toxicity and mesothelial cell reactions induced by potassium octatitanate fibers

- (TISMO) in the left thoracic cavity in A/J female mice. *Int J Toxicol* 2015; **34**: 325–35.
- 11 Renne R, Brix A, Harkema J *et al.* Proliferative and nonproliferative lesions of the rat and mouse respiratory tract. *Toxicol Pathol* 2009; **37**(7 Suppl): 5S–73S.
 - 12 Shield PW, Koivurinne K. The value of calretinin and cytokeratin 5/6 as markers for mesothelioma in cell block preparations of serous effusions. *Cytopathology* 2008; **19**: 218–23.
 - 13 Yokohira M, Kishi S, Yamakawa K *et al.* Napsin A is possibly useful marker to predict the tumorigenic potential of lung bronchiolo-alveolar hyperplasia in F344 rats. *Exp Toxicol Pathol* 2014; **66**: 117–23.
 - 14 Toyokuni S. Elucidation of asbestos-induced carcinogenesis and its application to prevention, diagnosis and treatment in relation to iron. *Jpn J Lung Cancer* 2009; **49**: 362–7.
 - 15 Sakamoto Y, Nakae D, Fukumori N *et al.* Induction of mesothelioma by a single intrascrotal administration of multi-wall carbon nanotube in intact male Fischer 344 rats. *J Toxicol Sci* 2009; **34**(1): 65–76.
 - 16 Takagi A, Hirose A, Nishimura T *et al.* Induction of mesothelioma in p53+/- mouse by intraperitoneal application of multi-wall carbon nanotube. *J Toxicol Sci* 2008; **33**(1): 105–16.
 - 17 Yokohira M, Nakano Y, Yamakawa K *et al.* Strain differences in pleural mesothelial cell reactions induced by potassium octatitanate fibers (TISMO) infused directly into the thoracic cavity. *Exp Toxicol Pathol* 2013; **65**: 925–32.
 - 18 Murphy FA, Poland CA, Duffin R *et al.* Length-dependent retention of carbon nanotubes in the pleural space of mice initiates sustained inflammation and progressive fibrosis on the parietal pleura. *Am J Pathol* 2011; **178**: 2587–600.
 - 19 Wang NS. The preformed stomas connecting the pleural cavity and the lymphatics in the parietal pleura. *Am Rev Respir Dis* 1975; **111**(1): 12–20.
 - 20 Kitamura Y, Umemura T, Kanki K *et al.* Lung as a new target in rats of 2-amino-3-methylimidazo[4,5-f]quinoline carcinogenesis: results of a two-stage model initiated with N-bis(2-hydroxypropyl)nitrosamine. *Cancer Sci* 2006; **97**: 368–73.
 - 21 Yamakawa K, Kuno T, Hashimoto N *et al.* Molecular analysis of carcinogen-induced rodent lung tumors: involvement of microRNA expression and Kralphas or Egfr mutations. *Mol Med Rep* 2010; **3**(1): 141–7.
 - 22 Ota Y, Imai T, Hasumura M *et al.* Prostaglandin synthases influence thyroid follicular cell proliferation but not carcinogenesis in rats initiated with N-bis(2-hydroxypropyl)nitrosamine. *Toxicol Sci* 2012; **127**: 339–47.
 - 23 Imai T, Cho YM, Hasumura M, Hirose M. Enhancement by acrylamide of N-methyl-N-nitrosourea-induced rat mammary tumor development-possible application for a model to detect co-modifiers of carcinogenesis. *Cancer Lett* 2005; **230**(1): 25–32.
 - 24 Shirai T, Kurata Y, Fukushima S, Ito N. Dose-related induction of lung, thyroid and kidney tumors by N-bis(2-hydroxypropyl)nitrosamine given orally to F344 rats. *Gan* 1984; **75**: 502–7.
 - 25 Beljan Perak R, Durdov MG, Capkun V *et al.* IMP3 can predict aggressive behaviour of lung adenocarcinoma. *Diagn Pathol* 2012; **7**: 165.
 - 26 Bishop JA, Sharma R, Illei PB. Napsin A and thyroid transcription factor-1 expression in carcinomas of the lung, breast, pancreas, colon, kidney, thyroid, and malignant mesothelioma. *Hum Pathol* 2010; **41**(1): 20–5.
 - 27 Stoll LM, Johnson MW, Gabrielson E, Askin F, Clark DP, Li QK. The utility of napsin-A in the identification of primary and metastatic lung adenocarcinoma among cytologically poorly differentiated carcinomas. *Cancer Cytopathol* 2010; **118**: 441–9.
 - 28 Yokohira M, Yamakawa K, Nakano Y *et al.* Immunohistochemical characteristics of surfactant proteins a, B, C and d in inflammatory and tumorigenic lung lesions of f344 rats. *J Toxicol Pathol* 2014; **27**: 175–82.
 - 29 Kadivar M, Boozari B. Applications and limitations of immunohistochemical expression of “Napsin-A” in distinguishing lung adenocarcinoma from adenocarcinomas of other organs. *Appl Immunohistochem Mol Morphol* 2012; **21**: 191–5.
 - 30 Masai K, Tsuta K, Kawago M *et al.* Expression of squamous cell carcinoma markers and adenocarcinoma markers in primary pulmonary neuroendocrine carcinomas. *Appl Immunohistochem Mol Morphol* 2012; **21**: 292–7.
 - 31 Doglioni C, Dei Tos AP, Laurino L *et al.* Calretinin: a novel immunocytochemical marker for mesothelioma. *Am J Surg Pathol* 1996; **20**: 1037–46.
 - 32 Taquahashi Y, Ogawa Y, Takagi A, Tsuji M, Morita K, Kanno J. Improved dispersion method of multi-wall carbon nanotube for inhalation toxicity studies of experimental animals. *J Toxicol Sci* 2013; **38**: 619–28.